CHEMISTRY
A EUROPEAN JOURNAL

DOI: 10.1002/chem.200600624

Silica Nanoparticles for Fluorescence Sensing of Zn^{II}: Exploring the Covalent Strategy

Pierluigi Teolato,[a] Enrico Rampazzo,[a] Maria Arduini,[a] Fabrizio Mancin,*[a] Paolo Tecilla,[b] and Umberto Tonellato[a]

Abstract: Silica nanoparticles (about 15 nm diameters), which contain a derivative of 6-methoxy-8-(*p*-toluensulfonamido)-quinoline (TSQ) as a Zn^{II} fluorescent probe covalently linked to the silica network, were prepared and studied as Zn^{II} fluorescent chemosensors. The systems selectively detect Zn^{II} ions in water rich solutions with a submicromolar sensitivity: 0.13 μM concentrations of Zn^{II} can be measured with the only interference of Cu^{II} and Cd^{II} ions. Compared with free TSQ, the nanoparticles based systems have the advantage that they can be employed in aqueous solutions without aggregation problems while at the same time, they maintain a similar Zn^{II} affinity and sensing ability. Addition of a second, substrate insensitive, fluorophore to the particles leads to the realization of a ratiometric sensor.

Keywords: fluorescent probes · nanoparticles · sensors · zinc

Introduction

Fluorescence chemical sensing involves the use of synthetic photoactive receptors to signal the presence of selected substrates by the variation of their fluorescence emission.[1] These tools are nowadays well established and widespread in several fields.[2] Indeed, such systems are typically simple to use, selective, sensitive and, most important, they allow measuring the analyte concentration with high response rate and spatial resolution. For these reasons, they are attracting increasing attention particularly in the intracellular monitoring of selected species in medical and biochemical applications.[1e,f] Recently, the inclusion of fluorescent chemosensors within nanoparticles, proposed by Kopelman and Rosenzweig and their co-workers, has emerged as an attractive new strategy for intracellular non-invasive real-time analysis.[3] These water-soluble nanoparticles, dubbed PEBBLEs (Probes Encapsulated By Biologically Located Embedding), are based on matrices of cross-linked polymers (e.g. polyacrilamide, polydecylmethacrylate, sol–gel silica) with a fluorescent chemosensor embedded and not linked to the polymer.[3a,b] These matrices have been used to make sensors for pH, metal ions, as well as for some non ionic species. The small size of such nanosensors (from 20 to 600 nm) still enables their non-invasive insertion into a living cell as in the case of molecular systems. The semipermeable and transparent nature of the matrix allows the interaction of the analyte with the indicator dye thus giving rise to a change of the emitted fluorescence. Moreover, when compared with the "naked" chemosensor, the nanoparticle can shelter the indicator from interferences, such as protein or membrane binding, also minimizing its toxicity. Intrinsic solubility of the chemosensor into aqueous solutions can be neglected, since it is taken up and transported by the nanoparticle. Finally, directing molecules can be attached to the particles surface, capable to confer to the nanosystems the ability to target only selected tissues or cells.

After those first reports, nanoparticles of different kinds, from polymers to quantum dots, have been used to investigate new strategies for the realization of fluorescent chemosensors.[4] We have recently introduced the chemical modification of silica nanoparticles for the preparation of self-organized multicomponent chemosensors.[5] In our approach, a fluorophore and a metal ion ligand are firstly modified by the conjugation with an alkoxysilane moiety and then covalently linked to the nanoparticle. Grafting of the two sensor components on the nanoparticle ensures their spatial prox-

[a] Dr. P. Teolato, Dr. E. Rampazzo, Dr. M. Arduini, Dr. F. Mancin, Prof. U. Tonellato
Dipartimento di Scienze Chimiche and CNR-ITM
Università di Padova, via Marzolo 1
35131 Padova (Italy)
Fax: (+39) 049-827-5239
E-mail: fabrizio.mancin@unipd.it

[b] Prof. P. Tecilla
Dipartimento di Scienze Chimiche
Università di Trieste, via Giorgieri 1
34127 Trieste (Italy)

imity and the binding of the metal ion, namely Cu^{II} ions, to the ligand results in a through space interaction with the dye which generates the signal. A similar approach has then been extended to different kinds of nanoparticles;[4a,b] among them those based on silica are particularly attracting as they are easy to make, water soluble, transparent to light and they can be easily engineered in compartments, where different species can be located to perform different functions. However, examples of silica nanoparticle based chemosensors are quite scarce and all devoted to the detection of fluorescence quenching species, namely molecular oxygen[6] and Cu^{II} ions.[4e,5a–c] Moreover, the sensing device is usually embedded in the nanoparticle core and is not covalently linked to the silica backbone. However, simple entrapping often results in leakage of the sensor and, in any case, prevents the engineering of the nanoparticles in chemically different compartments.

Moving from these considerations we have started a research aimed to the realization of nanosized chemosensors in which the sensing element is chemically bound to the silica nanoparticles with the final scope to obtain robust systems able to detect a wide range of substrates. In this paper, we describe our first results in the ratiometric detection of the photophysically inert Zn^{II} ion with good selectivity and sensitivity.

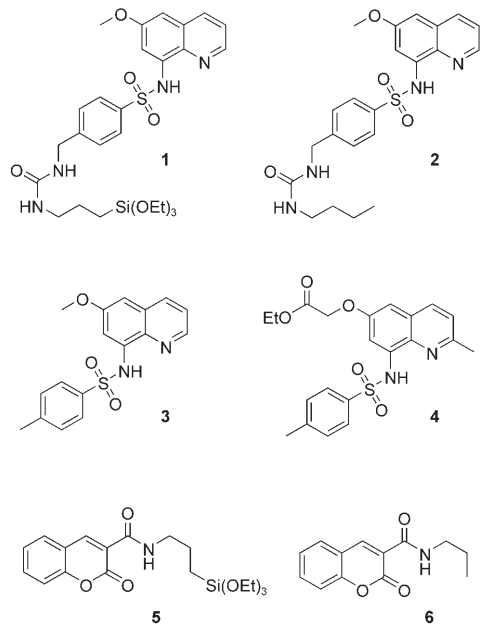

Results and Discussion

The synthetic procedure to prepare nearly monodisperse silica nanoparticles by condensation of tetralkoxysilanes in ammonia, water and ethanol solutions is known since the late 60s from the work of Stöber and subsequently of Van Blaaderen.[7,8] In early 90s, a modification of this procedure was proposed by Van Blaaderen in order to prepare covalently dye-doped silica nanoparticles.[9] It involves copolymerization of the tetralkoxysilane with a trialkoxysilane derivative of the dye. Later on, new procedures aimed at embedding organic molecules avoiding their chemical modification were reported.[10] They rely on the use of either reversed or normal micelles as "nanoreactors" where the polymerization reaction occurs involving the entrapment of the dopant distributed within the aggregate. However, such surfactant based methods require further workup in order to separate the surfactant from the particles; moreover, leaching of the included molecules from the particles can hardly be ruled out.

On the basis of such premises, we selected the 6-methoxy-8-(*p*-toluensulfonamido)-quinoline (TSQ, **3**, see below) as the active unit for the preparation of Zn^{II} sensing silica nanoparticles via the Stöber–Van Blaaderen procedure. TSQ and the closely related Zinquin (**4**, see below) are among the most popular intracellular Zn^{II} fluorescent probes actually in use.[1e,f,11] Derivative **1** was designed in order to attach to the molecule the triethoxysilane group, which is essential for the grafting to the particles silica network, without perturbing the fluoroionophore aromatic system. Synthesis of **1** was obtained in four steps (Scheme 1) from commercially available 6-methoxy-8-amino-quinoline (**7**) and 4-bromomethyl-benzensulfonyl chloride (**8**). Condensation of the two compounds in CH_2Cl_2 in the presence of pyridine afforded 6-methoxy-8-(4-(bromomethyl)benzensulfonamido)-quinoline (**9**), which was subsequently converted to the corresponding azide **10** by reaction with NaN_3 in DMF. Catalytic hydrogenation of **10**, using Pd on carbon, yielded amine **11** which was converted to **1** by condensation with 3-triethoxysilyl-propyl isocyanate. Following the same procedure, derivative **2**, which lacks the alkoxysilane group, was also prepared as reference compound.

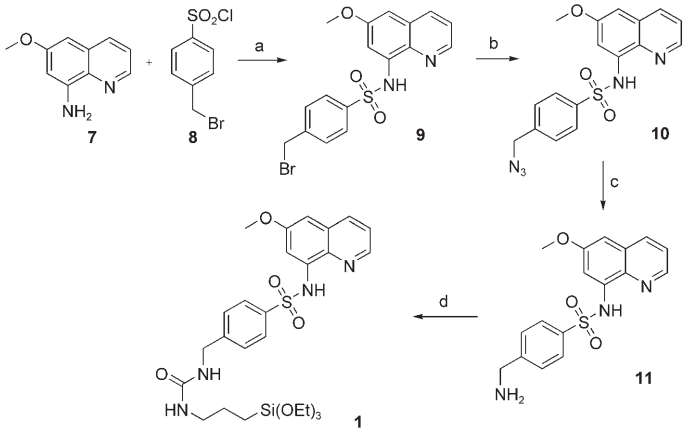

Scheme 1. Synthesis of fluoroionophore **1**. a) pyridine, dichloromethane, 0 °C; b) sodium azide, DMF, RT; c) H_2, Pd/C, methanol, RT; d) 3-(triethoxysiliyl)-propyl isocianate, tetrahydrofuran, −10 °C.

Compound **2** and the parent compound **3** are sparingly soluble in water and aggregation was detected from the absorption spectra even at low concentrations. For these rea-

sons, the following experiments were performed in 1:1 water/ethanol solutions. As expected, the photophysical properties of **2** are similar to those of **3**. The absorption spectra (Figure 1a) are almost identical and display two

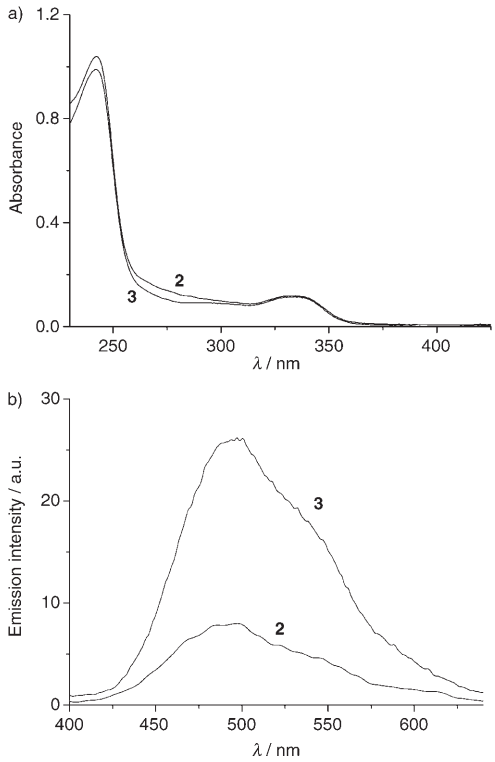

Figure 1. a) Absorption and b) emission spectra of fluoroionophores **2** and **3** in ethanol/water 1:1, pH 7.0. Conditions: [dyes] = 2.44×10^{-5} M, HEPES buffer 0.05 M, λ_{exc} = 340 nm, 25 °C.

bands at 245 and 335 nm. The emission spectra (Figure 1b) are very weak for both the compounds with maxima at 490 nm, but the intensity in the case of **2** is about three times lower than that of **3**. Quenched emission of 8-aminoquinoline derivatives is usually attributed to an intramolecular proton transfer coupled with a photo-induced excited-state electron transfer from the 8-amino residue to the quinoline nitrogen atom. Binding of metal ions usually inhibits such electron transfer resulting into a notable emission increase which is at the basis of their use as fluorescent chemosensors.[1e]

The effect of the addition of $Zn(NO_3)_2$ to a solution of **2** buffered at pH 7 is reported in Figure 2. The absorption bands undergo a red shift with the appearance of two new bands at 263 and 360 nm. Fluorescence spectra show a 30-fold increase of the emission accompanied by a 6 nm red-shift of the maximum. In the case of **3**, although the spectral changes are almost identical, the extent of the emission increases is about three times smaller. Fitting of the emission intensity versus metal ion concentrations reveals, as already reported in the case of similar Zinquin (**4**),[12] the formation of complexes with a 2:1 ligand to metal stoichiometry and

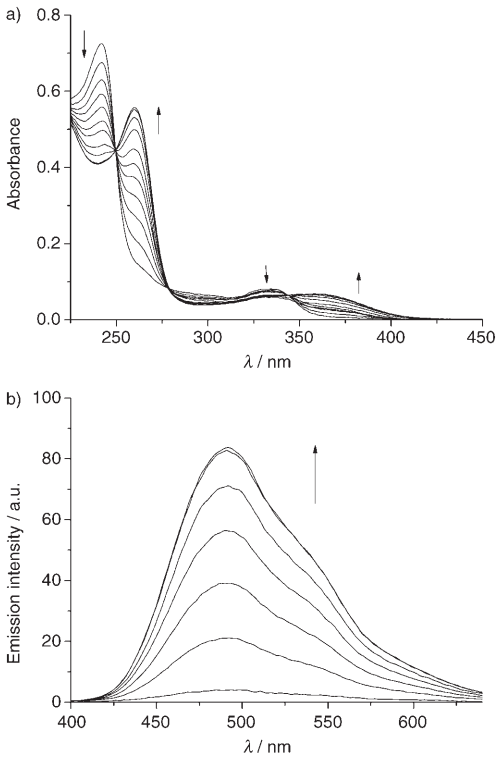

Figure 2. a) Absorption and b) emission spectra of fluoroionophore **2** in the presence of increasing $Zn(NO_3)_2$ concentrations (0–2.0×10^{-5} M) in ethanol/water 1:1, pH 7.0. Conditions: [dye] = 1.29×10^{-5} M, HEPES buffer 0.05 M, λ_{exc} = 340 nm, 25 °C.

with formation constants very similar for the two ligands (Table 1).

Table 1. Absorption, luminescence and apparent formation constant data relative to compounds **2**, **3** and their Zn^{II} complexes in water/ethanol 1:1 at 25 °C. (HEPES buffer 0.05 M).

	Absorption		Fluorescence		
	λ_{max} [nm]	ε_{max} [$M^{-1}cm^{-1}$]	λ_{max} [nm]	Φ[a]	logβ[b]
3	245	4.15×10^4	490	0.045	
	335	4.84×10^3			
3$_2$·Zn^{II}	263	7.41×10^4	496	0.194	11.0
	360	8.80×10^3			
2	244	4.40×10^4	490	0.015	
	336	4.95×10^3			
2$_2$·Zn^{II}	263	6.75×10^4	496	0.096	11.3
	360	8.51×10^3			

[a] Fluorescence quantum yield. [b] $\beta = [L_2{\cdot}Zn^{II}]/[L]^2[Zn^{II}]$.

Silica nanoparticles containing chemosensor **1** were prepared by co-condensation of a mixture of tetraethoxysilane (TEOS) and **1** in ethanol/water/ammonia at 25 °C. The molar ratio of **1** to TEOS in the reaction mixture was fixed at a value of 1:100, since greater amount of **1** in the reaction mixtures prevented the formation of the nanoparticles. The colloid solutions were purified by extensive ultrafiltration over a 10000 Dalton (~3 nm) cut-off membrane to eliminate unreacted species and hydrolyzed monomers.

The resulting particles were investigated by transmission electron microscopy (TEM, Figure 3a): the average diameter is 10.2 nm with a 2.5 nm polydispersity (24%). Dynamic light scattering (DLS) analysis yielded similar results indicating a 14.8 nm average diameter and a 4.8 nm (32%) polydispersity. DLS hydrodynamic diameters are usually found to be greater than those measured by TEM analysis: such effect has been ascribed to the shrinkage of the particles due to the microscope electron beam.[8] At any rate, the particles obtained are quite small, poorly spherical and barely monodisperse. Similar features are commonly observed in the case of silica particles with diameters smaller that 30 nm, when prepared with the Stöber synthesis.[8]

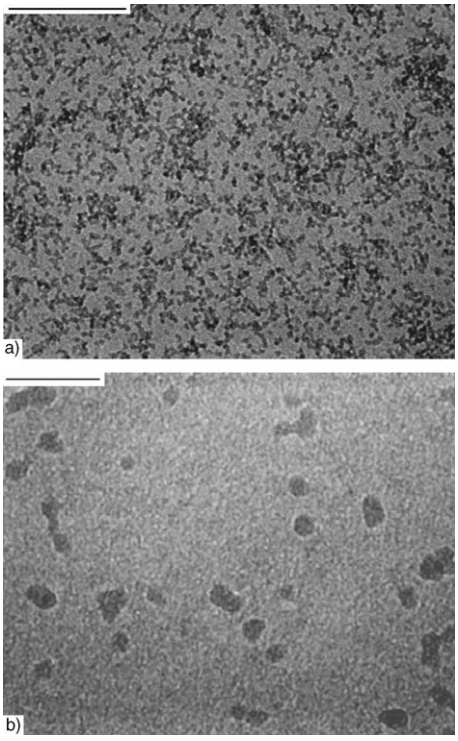

Figure 3. TEM images of a) **1**-doped and b) **1/5**-doped silica nanoparticles. Bars: a) 250 nm, b) 100 nm.

Absorption and emission spectra of a nanoparticles solution in 1:1 water/ethanol reveal the presence of the chemically linked fluoroionophore (Figure 4). However, in addition to the characteristic bands at 245 and 335 nm, two shoulders at 260 and 360 nm can be detected in the absorption spectrum (Figure 4a). These two bands are typical of the protonated form (or metal ion complexed) of the 6-methoxy-8-(benzensulfonamido)-quinoline derivatives. Therefore, in the absence of metal ions, it is probable that part of the fluoroionophore present within the nanoparticles is protonated by the acidic silanol groups of the silica network. The intensity ratio between the band at 245 and the shoulder at 260 nm indicates that about 30% of the fluoroionophore exists in the protonated form. Such hypothesis is further confirmed by the analysis of the emission spectra of the nanoparticles. The emission maximum is centred at 486 nm and the quantum yield is 0.12. This value is much higher than that of **2** in water/ethanol solutions and such effect could be ascribed at least partly to the protonation of part of the photoactive units. Decreased solvent quenching of the emission due to the inclusion in the nanoparticle could also be involved in the high quantum yield observed. The embedding of **1** within the nanoparticles is confirmed by the fluorescence anisotropy value of 0.10, compatible with a low mobility of the dyes due to the grafting to the nanoparticles.

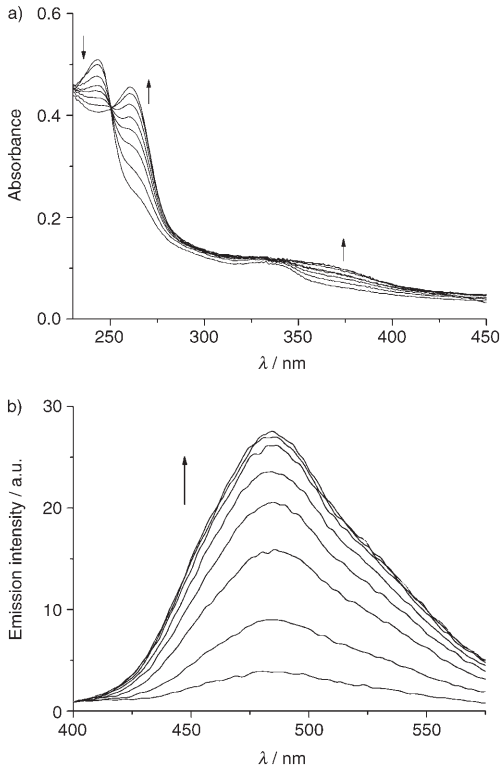

Figure 4. a) Absorption and b) emission spectra of a solution of **1** containing nanoparticles in the presence of increasing $Zn(NO_3)_2$ concentrations (0–2.0×10^{-5} M) in ethanol/water 1:1, pH 7.0. Conditions: [dye] = 1.4×10^{-5} M, HEPES buffer 0.05 M, λ_{exc} = 340 nm, 25 °C.

The effect of the addition of Zn^{II} ions to a **1** doped nanoparticles solution is reported also in Figure 5. Spectral modifications closely resemble those observed in the case of free chemosensors **2** and **3**. On the one hand, the absorption band at 245 nm decreases while two new maxima appear at 260 and 360 nm, on the other hand, the emission band undergoes a six-fold intensity increase. Such increment is smaller than that recorded using **2** and this is probably due to the higher quantum yield of the uncomplexed sensor embedded in the particles: as a consequence, the effect of the complexation on the emission increase is less dramatic. The concentration of fluoroionophores present in the particles solution was roughly estimated, using the molar extinction coefficient measured for **2** in the same solvent, to be 1.4×10^{-5} M. The emission intensity versus Zn^{II} concentration profile (Figure 5) was fitted using models involving either a 1:1,

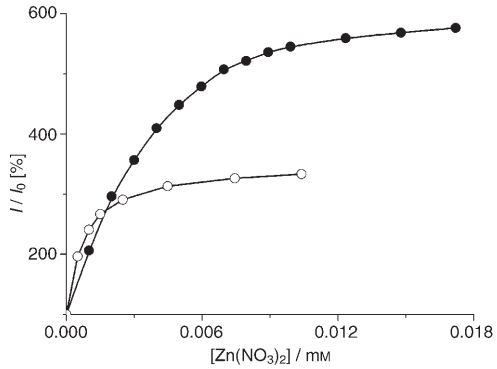

Figure 5. Spectrofluorimetric titration with $Zn(NO_3)_2$ of a solution of **1** containing nanoparticles in 1:1 (●, [dye] = 1.4×10^{-5} M) and 9:1 (○, [dye] = 2.8×10^{-6} M) water/ethanol solutions at pH 7.0. Conditions: HEPES buffer 0.05 M, 25 °C, λ_{exc} = 340 nm, λ_{em} = 490 nm.

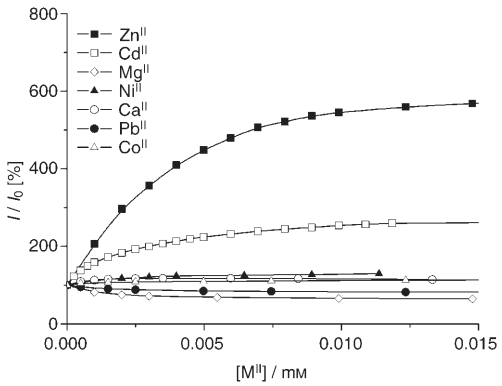

Figure 6. Spectrofluorimetric titration of a solution of **1** containing nanoparticles in 1:1 water/ethanol solutions at pH 7.0 with $CaCl_2$, $MgCl_2$, $Zn(NO_3)_2$, $Cd(NO_3)_2$, $CoCl_2$, $Ni(NO_3)_2$, and $Pb(NO_3)_2$. Conditions: [dye] = 1.4×10^{-5} M, HEPES buffer 0.05 M, 25 °C, λ_{exc} = 340 nm, λ_{em} = 490 nm.

2:1 (or both) ligand to metal complexation stoichiometries. Reliable results were obtained only in the case of the 2:1 model. The fit yielded a logβ value of 11.1 and a ligand concentration of 0.9×10^{-5} M. When this value is compared with the total concentration of **1** determined by UV/Vis analysis, it comes out that only 65% of the sensor units are available for the interaction with the Zn^{II} ions. Such result is in good agreement with the previous assessment of the presence of a 30% fraction of protonated sensor units, hence unavailable for Zn^{II} complexation, in the metal-free particles. The finding of a 2:1 ligand to metal complexation stoichiometry also in the case of the dye-doped nanoparticle is somehow surprising, since one could expect that the covalent linking of the subunits of **1** to the silica network should decrease their mobility and prevent the formation of 2:1 complexes. However, aggregation of organic fluorophores to form domains within silica particles has been already reported[13] and could be at the origin of the observed binding stoichiometries.

Beside the speculation of the internal structure of the nanoaparticles, their sensing efficiency must be highlighted. If the amount of Zn^{II} needed to produce a 25% increase of the initial fluorescence emission is taken as reference detection limit, Zn^{II} concentration down to 2.6×10^{-7} M can be detected. Moreover, unlike the free sensors **2** and **3**, particles containing **1** can be used in mixed solutions with high percentage of water. Figure 5 reports also the titration profile of a particles solution in 9:1 water/ethanol. The sensing efficiency is similar to that obtained in 1:1 water/ethanol. A saturation three-fold emission increase is observed and the Zn^{II} concentration which produces a 25% increase of the initial fluorescence emission is 1.3×10^{-7} M.

The selectivity of **1** containing nanoparticles chemosensor was tested using several divalent metal ions. The titrations profiles are reported in Figure 6. Beside Zn^{II}, only Cd^{II} produces a two-fold emission increase, while Cu^{II} causes a 80% quenching of the initial emission (not shown). All other metal ions tested produced no or very little variations of the particles emission. This result is in line with the reported ability of 6-methoxy-8-(benzensulfonamido)-quinoline derivatives to selectivity sense Zn^{II} ions with interferences from Cu^{II} and, to a minor extent, from Cd^{II}, which, however, are not present in relevant amounts in biological systems.[14]

One of the main advantages of the PEBBLE approach is the possibility to convert off–on sensors into ratiometric sensors by simply adding to the system a fluorophore that is indifferent to the substrate and produces a constant reference signal.[3,6] In order to investigate such possibility, we prepared nanoparticles containing both the active fluoroionophore **1** and the indifferent coumarine derivative **5** (see above) chemically-linked to the silica network. The amount of the two dyes was fixed at 0.5% each with respect of TEOS. DLS analysis of the purified particles yielded a 17 nm diameter, while TEM confirmed the presence particles of about 10–15 nm diameter (Figure 3b). However, we were unable to obtain TEM pictures with a suitable quality for dimensional analysis. Absorption spectra of the nanoparticles solutions confirm the presence of both **1** and **5** (Figure 7a), with the characteristic absorption maxima at 244 and 334 nm (due to **1**) and 295 nm (due to **5**, see Figure 7b). The ratio between absorption intensities at 244 and 295 nm indicates that the two molecules are present in similar amounts within the particles.

Also the emission spectra show the maxima characteristic of the two species **1** and **5** at 486 and 410 nm, respectively (Figure 7a); contribute of the sole dye **1** can be observed upon excitation at 370 nm, where **5** absorption is negligible.

Titration of silica particles containing both **1** and **5** with Zn^{II} resulted in the usual six-fold increase of the emission of **1** units (Figure 8b). Almost no difference in the titration profiles was detected when excitation was set at 295 or 370 nm, confirming that the second fluorophore does not interfere with the response of the fluoroionophore. Moreover, when excitation is set at 295 nm, the emission band of **5** at 410 nm remains constant in intensity and position through the whole titration (Figure 8a), acting as an internal reference and validating the particles as ratiometric sensors.

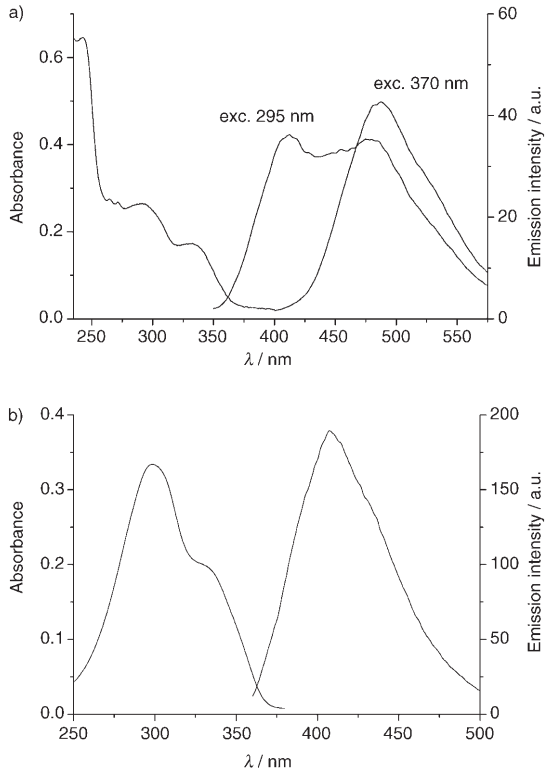

Figure 7. Absorption and emission spectra of a) solution of **1** and **5** containing nanoparticles (A, [**1**] = 1.5×10^{-5} M, [**5**] = 1.2×10^{-5} M) and of a solution of dye **6** (B, [**6**] = 3.0×10^{-5} M) in ethanol/water 1:1, pH 7.0. Conditions: HEPES buffer 0.05 M, 25 °C.

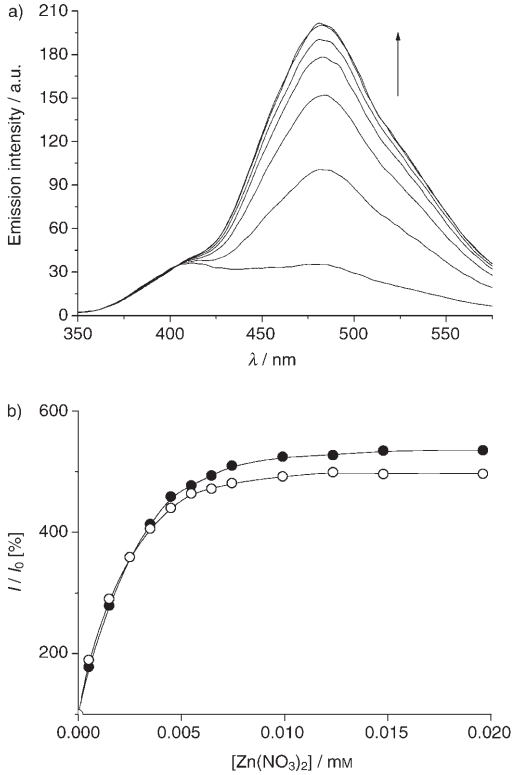

Figure 8. a) Emission spectra (λ_{exc} = 295 nm) of a solution of **1** and **5** containing nanoparticle in the presence of increasing $Zn(NO_3)_2$ concentrations (0–2.0×10^{-5} M). b) Emission intensity versus Zn^{II} concentration of the same solution upon excitation at 295 nm (●) and 370 nm (○). Conditions: ethanol/water 1:1, [**1**] = 1.5×10^{-5} M, [**5**] = 1.2×10^{-5} M, HEPES buffer 0.05 M ethanol/water 1:1 pH 7.0, 25 °C.

Conclusion

The main advantage of the use of silica nanoparticles compared with other materials in the development of fluorescent chemosensors is probably their rigidity. They do not swell or collapse by changing the solvent system and they present well defined compartments: surface, shells, mesopores that can be used to organize the functional species introduced in the particles to perform very complex functions.[15] In view of these features, the chemical functionalization of the nanoparticles appears to be a promising strategy if compared with the simple embedding of the active components in the nanoparticle. At least in principle, it can allow the precise localization of the selected species in the desired compartment and avoids leaking. On the other hand, the use of silica nanoparticles in fluorescence sensing, and particularly metal ion sensing, could suffer from some limitations regarding their permeability and non-specific binding of metal ions to the particles surface.[5c]

The results reported in the present study reveal that ratiometric Zn^{II} sensing is possible within chemically modified silica nanoparticles. Binding ability of the 6-methoxy-8-(benzensulfonamido)-quinoline units appears unaltered and the sensing efficiency observed is similar to that of free TSQ (**3**). In addition, nanoparticles embedding allows the use of water rich, and presumably also pure water, solutions.

The main limit of the systems presented in this work is the increased quantum yield of the particles embedded fluoroionophore, probably due to protonation of the dye by the acidic silanol groups. Such problem could be overcome by the passivation of the free silanol groups after particles preparation or by the use of ORMOSIL particles instead of the traditional silica ones. The instauration of communication effect between the embedded fluorophores, such as resonance energy transfer processes, could be used to increase the signalling efficiency of the sensors.[16] Finally, surface functionalization of the particles could increase their cell penetration ability.

Experimental Section

General: All commercially available solvents and reagents were used as received without further purification. TLC analyses were performed using Merck 60 F_{254} (0.25 mm) precoated silica gel glass plates and Machery–Nagel Poligram SIL G/UV_{254} precoated plastic sheets (0.25 mm). Preparative column chromatography was carried out on glass columns packed with Macherey–Nagel 60 (70–230 mesh) and on Merck Kieselgel 60, 0.063 mm silica gel. Petroleum ether b.p. range 40–60 °C.

NMR spectra were recorded with a Bruker AC 250F spectrometer. Chemical shifts are reported relative to tetramethylsilane as internal standard. Signals in NMR spectra are reported as follows: s = singlet; d

= doublet, t = triplet, q = quartet, qn = quintet, m = multiplet, b = broad. Multiplicity is given as usual. ESI-MS mass spectra were obtained with a Navigator ThermoQuest-Finningan mass spectrometer. Elemental analyses were performed by the Laboratorio di Microanalisi of the Department of Chemical Sciences of the University of Padova.

Transmission electron microscopy (TEM) experiments were performed at the CSPA of the University of Trieste. TEM images of the particles were obtained with a Philips EM 208 transmission electron microscope operating at 100 keV. Samples for TEM were prepared by spreading a drop of nanoparticles solution in ethanol (~5 mg mL^{-1}) onto standard carbon-coated copper grids (200 mesh). Dimensional analysis of nanoparticles from TEM images has been made with the Image J software.[17]

Dynamic light scattering (DLS) measurements were obtained with a Particle Sizing Systems Nicomp Model 370 correlator equipped with a thermostated cell holder and a Spectra Physics Series 2016 Ar laser operating at 488 nm. Hydrodynamic particles diameters were obtained from cumulant fits of the autocorrelation functions at 90° scattering angle.

UV/Vis absorption measurements were performed at 25 °C by means of Perkin–Elmer Lambda 16 and 45 spectrophotometers equipped with thermostated cell holders. Quartz cells with optical path length of 1 cm were used. Fluorescence spectra were recorded at 25 °C with a Perkin–Elmer LS-55 spectrofluorimeter equipped with a Hamamatsu R928 photomultiplier and thermostated cell holder, quartz cells with optical path length of 1 cm were used. Fluorescence quantum yields were determined standard of quinine sulphate in 0.05 M H_2SO_4 ($\Phi = 0.564$).

6-Methoxy-8-(*p*-toluensulfonamido)-quinoline (TSQ, **3**),[18] coumarin 3-carboxylic acid propylamide (**6**)[5c] and 3-triethoxysiliyl-1-(coumarin 3-carboxamide)-propane (**5**)[5c] were prepared according to reported procedures.

Spectrophotometric titrations: $Cu(NO_3)_2$, $Zn(NO_3)_2$, $Ni(NO_3)_2$, $CoCl_2$, $Fe(NO_3)_2$, $CdCl_2$, $Pb(NO_3)_2$, $CaCl_2$ and $MgCl_2$ were analytical grade products. Metal ion stock solutions were titrated against EDTA following standard procedures. Solution used during the spectrophotometric measurements and titrations were prepared using deionized water (R > 18 MΩ), obtained with a Milli-Q (Millipore) purification system and HPLC grade ethanol. The buffer 4-(2-hydroxyethyl)-1-piperazineethanesulfonic acid (HEPES, Alrich) was used as received and stock solutions (0.2 M) were prepared using Milli-Q water.

The total molar concentration of dye subunits in the nanoparticles ethanol suspensions resulting from ultrafiltration was determined from their absorbance using the ε values of the corresponding models in ethanol (**2**: 4.40×10^4 M^{-1}cm^{-1}, 244 nm; **6**: 1.52×10^4 M^{-1}cm^{-1}, 297 nm). The desired amount of such suspensions was then transferred in fluorescence quartz cells and ethanol, water and buffer were added to reach a final volume of 2 mL. The suspension was allowed to equilibrate until no variation of the emission spectrum were observed (usually an equilibration time of about 1 h was required), then small volumes (up to 50 μL) of concentrated metal ions solutions were added and the fluorescence or absorption spectra were recorded. Every experiment was repeated at least three time with reproducible results.

Fitting of the titration curves was performed with the software package Scientist 2.01.[19] A model involving the formation of 2:1 ligand to metal Zn^{II} complexes was used to estimate the Zn^{II} complexation strength (binding constants) and, in the case of the nanoparticles, the concentration of binding sites, the fit error being in each case less than 10%.

4-Bromomethyl-*N*-(6-methoxy-quinolin-8-yl)-benzenesulfonamide (9): 8-Amino-6-methoxy-quinoline hydrobromide (**7**, 221 mg, 0.84 mmol) was dissolved in CH_2Cl_2 (4 mL) under nitrogen atmosphere. The mixture was cooled in an acetone/dry ice bath and pyridine (24 μL, 3.0 mmol) was added. A solution of 4-bromomethyl-benzenesulfonyl chloride (**8**, 284 mg, 0.95 mmol) in CH_2Cl_2 (4 mL) was added dropwise. After addition of **8**, the reaction mixture became clear and turned into a deep yellow colour. The reaction mixture was stirred in the cooling bath for 20 min (TLC, CH_2Cl_2/petroleum ether/CH_3OH 10:1:0.5), then the solvent was removed by rotary evaporation and water and ice (30 mL) were added. The resulting precipitate was filtered out and dissolved in CH_2Cl_2 (100 mL). The organic solution was extracted with 1 M HCl (100 mL), the resulting aqueous phase was further extracted with CH_2Cl_2 (2×75 mL) and the combined organic phases were dried with Na_2SO_4 and evaporated under reduced pressure. The crude product was finally purified by flash column chromatography (silica gel, CH_2Cl_2/petroleum ether 5:3→8:3) to provide **9** (336 mg, 98%) as a white solid. ^{1}H NMR (250 MHz, $CDCl_3$, 25 °C): δ = 9.23 (brs, 1H; NH), 8.57 (dd, ^3J = 4.2, ^4J = 1.6 Hz, 1H; H^2 *Quin*), 7.96 (dd, ^3J = 8.8, ^4J = 1.6 Hz, 1H; H^4 *Quin*), 7.90 (d, ^3J = 6.8 Hz, 2H; H^3 and H^4 *Benz*), 7.49 (d, ^4J = 2.5 Hz, 1H; H^7 *Quin*), 7.39 (d, ^3J = 6.8 Hz, 2H; H^2 and H^6 *Benz*), 7.35 (dd, ^3J = 8.8, ^3J = 4.2 Hz, 1H; H^3 *Quin*), 6.71 (d, ^4J = 2.5 Hz, 1H; H^5*Quin*), 4.37 (s, 2H; -CH_2Br), 3.87 ppm (s, 3H; CH_3O-).

4-Azidomethyl-*N*-(6-methoxy-quinolin-8-yl)-benzenesulfonamide (10): NaN_3 (107 mg, 1.64 mmol) was added to a solution of **9** (336 mg, 0.82 mmol) in DMF (7 mL). The mixture was stirred overnight, then the solvent was evaporated and the residue was dissolved in CH_2Cl_2 (100 mL). The organic solution was extracted with water (70 mL), the resulting aqueous phase was further extracted with CH_2Cl_2 (2×50 mL) and the combined organic phases were dried with Na_2SO_4. The solvent was evaporated under reduced pressure to yield **10** (279 mg, 91%) as a white solid. The presence of the characteristic peak at 2096 cm^{-1} in the FT-IR spectrum confirmed the presence of the N_3 group. ^{1}H NMR (250 MHz, $CDCl_3$, 25 °C): δ = 9.23 (brs, 1H; NH), 8.57 (dd, ^3J = 4.2, ^4J = 1.6 Hz, 1H; H^2 *Quin*), 7.97 (dd, ^3J = 8.5, ^4J = 1.6 Hz, 1H; H^4 *Quin*), 7.93 (d, ^3J = 8.5 Hz, 2H; H^3 and H^4 *Benz*), 7.49 (d, ^4J = 2.5 Hz, 1H; H^7 *Quin*), 7.35 (dd, ^3J = 8.5, ^3J = 4.2 Hz, 1H; H^3 *Quin*), 7.32 (d, ^3J = 8.5 Hz, 2H; H^2 and H^6 *Benz*), 6.71 (d, ^4J = 2.5 Hz, 1H; H^5 *Quin*), 4.33 (s, 2H; -CH_2N_3), 3.87 ppm (s, 3H; CH_3O-).

4-Aminomethyl-*N*-(6-methoxy-quinolin-8-yl)-benzenesulfonamide (11): A solution of **10** (279 mg, 0.75 mmol) in CH_2Cl_2 (3 mL) was poured into CH_3OH (25 mL), 10% Pd on carbon (50 mg) was added to the stirred resulting suspension and hydrogen was bubbled for 2 h (TLC $CHCl_3$/CH_3OH/$NH_{3(aq)}$ 15:4:0.2). The reaction mixture was then diluted with CH_3OH (50 mL) and filtered on a Celite pad. The solvent was evaporated and crude product was finally purified by flash column chromatography (silica gel, CH_2Cl_2, then CH_2Cl_2/MeOH 25:1 and finally CH_2Cl_2/MeOH/$NH_{3(aq)}$ 25:1:0.08) to provide **11** (119 mg, 46%) as a white solid. ^{1}H NMR (250 MHz, $CDCl_3$, 25 °C): δ = 8.57 (dd, ^3J = 2.8, ^4J = 1.6 Hz, 1H; H^2 *Quin*), 7.94 (dd, ^3J = 8.2, ^4J = 1.2 Hz, 1H; H^4 *Quin*), 7.87 (d, ^3J = 8.5 Hz, 2H; H^3 and H^4 *Benz*), 7.47 (d, ^4J = 2.5 Hz, 1H; H^7 *Quin*), 7.35 (dd, ^3J = 8.2, ^3J = 2.8 Hz, 1H; H^3 *Quin*), 7.33 (d, ^3J = 8.2 Hz, 2H; H^2 and H^6 *Benz*), 6.69 (d, ^4J = 2.5 Hz, 1H; H^5 *Quin*), 3.86 (s, 3H; CH_3O-), 3.58 ppm (s, 2H; -CH_2NH_2).

4-(3-(3-Triethoxysilyl)propyl-ureidomethyl)-*N*-(6-methoxy-quinolin-8-yl)-benzenesulfonamide (1): A solution of (3-triethoxysilyl)-propyl isocyanate (90 μL, 0.35 mmol) in THF (10 mL) was added dropwise to a suspension of **11** (119 mg, 0.35 mmol) in THF (20 mL) at −10 °C. When all the reagents were consumed (TLC $CHCl_3$/petroleum ether/CH_3OH 10:1:0.5), the solvent was evaporated to provide **2** (63 mg. 98%) as a white solid. ^{1}H NMR (250 MHz, [D$_4$]THF, 25 °C): δ = 9.33 (brs, 1H; -$NHSO_2$-), 8.58 (dd, ^3J = 4.2, ^4J = 1.5 Hz, 1H; H^2 *Quin*), 8.04 (dd, ^3J = 8.2, ^4J = 1.5 Hz, 1H; H^4 *Quin*), 7.84 (d, ^3J = 8.5 Hz, 2H; H^3 and H^4 *Benz*), 7.51 (d, ^4J = 2.8 Hz, 1H; H^7 *Quin*), 7.37 (dd, ^3J = 8.2, ^3J = 4.2 Hz, 1H; H^3 *Quin*), 7.31 (d, ^3J = 8.5 Hz, 2H; H^2 and H^6 *Benz*), 6.84 (d, ^4J = 2.5 Hz, 1H; H^5 *Quin*), 5.49 (brs, 1H; -NH-), 5.18 (brs, 1H; -NH-), 4.25 (m, 2H; -C*H*$_2$NH-), 3.86 (s, 3H; CH_3O-), 3.78, (q, ^3J = 6.8 Hz, 6H; -OC*H*$_2$CH$_3$), 3.07 (brt, ^3J = 6.8 Hz, 2H; -C*H*$_2$CH$_2$CH$_2$Si-), 1.52 (bqn, ^3J = 6.8 Hz, 2H; -C*H*$_2$CH$_2$Si-), 1.17 (t, ^3J = 6.8 Hz, 9H; -OCH$_2$C*H*$_3$), 0.55 ppm (m, 2H; -CH$_2$Si-); ^{13}C NMR (69.9 MHz, [D$_4$]THF, 25 °C): δ = 159.2, 158.73, 148.0, 146.9, 136.3, 136.1, 135.9, 130.5, 128.4, 128.0, 125.9, 123.3, 108.4, 100.3, 58.9, 55.8, 30.8, 25.0, 19.1, 18.8, 8.5 ppm; ESI-MS: *m*/*z* (%): 591.0 (30) [*M*+H$^+$], 613.3 (100) [*M*+Na$^+$], 629.3 (5) [*M*+K$^+$]; elemental analysis calcd (%) for $C_{27}H_{38}N_4O_7SSi$: C 54.89, H 6.48, N 9.48, S, 5.43; found: C 54.57, H 6.59, N 9.27, S 5.60.

4-((3-Butyl-ureido)-methyl)-*N*-(6-methoxy-quinolin-8-yl)-benzenesulfonamide (2): A solution of butyl isocyanate (16 μL, 0.15 mmol) in THF (5 mL) was added dropwise to a suspension of **11** (50 mg, 0.15 mmol) in THF (15 mL) at −10 °C. When all the reagents were consumed (TLC $CHCl_3$/petroleum ether/CH_3OH 10:1:0.5) the solvent was evaporated to

provide **1** (199 mg, 97%) as a white solid. ^{1}H NMR (250 MHz, [D$_4$]THF, 25°C): δ = 8.58 (dd, ^3J = 4.2, ^4J = 1.5 Hz, 1H; H^2 *Quin*), 8.04 (dd, ^3J = 8.2, ^4J = 1.5 Hz, 1H; H^4 *Quin*), 7.82 (d, ^3J = 8.5 Hz, 2H; H^3 and H^4 *Benz*), 7.52 (d, ^4J = 2.8 Hz, 1H; H^7 *Quin*), 7.37 (dd, ^3J = 8.2, ^3J = 4.2 Hz, 1H; H^3 *Quin*), 7.22 (d, ^3J = 8.5 Hz, 2H; H^2 and H^6 *Benz*), 6.84 (d, ^4J = 2.5 Hz, 1H; H^5 *Quin*), 5.83 (brt, 1H; -NH-), 5.47 (brt, 1H; -NH-), 4.18 (d, 2H, ^3J = 4 Hz; -C*H*$_2$NH-), 3.83 (s, 3H; CH$_3$O-), 3.03 (q, ^3J = 6.2 Hz, 2H; -C*H*$_2$CH$_2$CH$_2$CH$_3$), 1.28 (m, 4H; -CH$_2$C*H*$_2$C*H*$_2$CH$_3$), 0.86 ppm (t, 3H, ^3J = 6.8 Hz; -CH$_2$C*H*$_3$); ESI-MS: *m*/*z* (%): 443.2 (40) [*M*+H$^+$], 465.3 (100) [*M*+Na$^+$]; elemental analysis calcd (%) for C$_{22}$H$_{26}$N$_4$O$_4$S: C 59.71, H 5.92, N 12.66, S 7.25; found: C 59.36, H 6.08, N 12.49, S 7.22.

Preparation of the dye doped silica nanoparticles: Preparation of nanoparticles containing **1** is reported as an example of general procedure. Particles containing **1** and **5** were prepared by following the same procedure with different amounts of the organosilane reagents, namely 0.002 mmol each. Compound **1** (2.4 mg, 0.004 mmol) was dissolved in ethanol (20 mL), and to this solution TEOS (100 μL, 0.43 mmol) and a 29% ammonia water solution (0.6 mL) were added. The reaction mixture was thermostated at 25°C and vigorously stirred for 16 h. The resulting nanoparticles suspension was diluted to 70 mL with ethanol and transferred into a 75 mL Amicon Ultrafiltration Cell, equipped with a 10 kDa regenerated cellulose membrane and an 800 mL solvent reservoir. The mixture was extensively ultra-filtrated, under a pressure of 4 bar, until the UV/Vis spectrum of the filtrate showed the absence of **1** absorption. The retentate solution was finally filtrated through a 0.45 μM filter membrane.

Acknowledgements

The authors thank Mr. Claudio Gamboz and Prof. Maria Rosa Soranzo (CSPA, University of Trieste) for kind help with TEM analysis. Financial support for this research has been partly provided by the Ministry of Education, University and Research (MIUR contracts 2003030309 and 2003037580) and by University of Padova (University Research Project CPDA034893).

[1] a) *Fluorescent Chemosensors for Ion and Molecule Recognition* (Ed.: A. W. Czarnik), ACS Symposium Series 538, American Chemical Society, Washington DC, **1993**; b) A. P. de Silva, H. Q. N. Gunaratne, T. Gunnlaugsson, A. J. M. Huxley, C. P. McCoy, J. T. Rademacher, T. E. Rice, *Chem. Rev.* **1997**, *97*, 1515–1566; c) *Special Issue on "Luminescent Sensors"* (Ed.: L. Fabbrizzi), *Coord. Chem. Rev.* **2000**, 2005, Issue 1; d) K. Rurack, U. Resch-Genger, *Chem. Soc. Rev.* **2002**, *31*, 116–127; e) P. Jiang, Z. Guo, *Coord. Chem. Rev.* **2004**, 248, 205–229; f) K. Kikuchi, K. Komatsu, T. Nagano, *Curr. Opin. Chem. Biol.* **2004**, *8*, 182–191; g) *Special Issue on "Fluorescent Sensors"* (Eds.: A. P. de Silva, P. Tecilla), *J. Mater. Chem.* **2005**, 15, Issues 27–28; h) J. F. Callan, A. P. de Silva, D. C. Magri, *Tetrahedron* ***2005****, 61*, 8551–8588; i) L. Prodi, *New J. Chem.* **2005**, *29*, 20–31.

[2] *The Handbook: a Guide to Fluorescent Probes and Labeling Technologies* (Ed.: M. T. Spence), 10th ed., Invitrogen Corp., **2005**.

[3] a) S. M. Buck, Y. E. L. Koo, E. Park, H. Xu, M. Brasuel, M. A. Philbert, R. Kopelman, *Curr. Opin. Chem. Biol.* **2004**, *8*, 540–546; b) S. M. Buck, H. Xu, M. Brasuel, M. A. Philbert, R. Kopelman, *Talanta* **2004**, *63*, 41–59; c) J. Lu, Z. Rosenzweig, *Fresenius J. Anal. Chem.* **2000**, *366*, 569–575.

[4] a) K. M. Gattás-Asfura, R. M. Leblanc, *Chem. Commun.* **2003**, 2684–2685; b) R. Méallet-Renault, R. Pansu, S. Amigoni-Gerbier, C. Lampent, *Chem. Commun.* **2004**, 2344–2345; c) W. J. Jin, M. T. Fernández-Argüelles, J. M. Costa-Fernández, R. Pereiro, A. Sanz-Medel, *Chem. Commun.* **2005**, 883–885; d) T. Jin, F. Fujii, H. Sakata, M. Tamura, M. Kinjo, *Chem. Commun.* **2005**, 4300–4302; e) M. Montalti, L. Prodi, N. Zaccheroni, *J. Mater. Chem.* **2005**, *15*, 2810–2814.

[5] a) E. Brasola, F. Mancin, E. Rampazzo, P. Tecilla, U. Tonellato, *Chem. Commun.* **2003**, 3026–3027; b) E. Rampazzo, E. Brasola, S. Marcuz, F. Mancin, P. Tecilla, U. Tonellato, *J. Mater. Chem.* **2005**, *15*, 2687–2696; c) M. Arduini, S. Marcuz, M. Montolli, E. Rampazzo, F. Mancin, S. Gross, L. Armelao, P. Tecilla, U. Tonellato, *Langmuir* **2005**, *21*, 9314–9321; d) F. Mancin, E. Rampazzo, P. Tecilla, U. Tonellato, *Chem. Eur. J.* **2006**, *12*, 1844–1854.

[6] a) H. Xu, J. W. Aylott, R. Kopelman, T. J. Miller, M. A. Philbert, *Anal. Chem.* **2001**, *73*, 4124–4133; Y-E. L. Koo, Y. Cao, R. Kopelman, S. M. Koo, M. Brasuel, M. A. Philbert, *Anal. Chem.* **2004**, *76*, 2498–2505.

[7] W. Stöber, A. Fink, E. Bohn, *J. Colloid Interface Sci.* **1968**, *26*, 62–69.

[8] a) A. Van Blaaderen, A. P. M. Kentgens, *J. Non-Cryst. Solids* **1992**, *149*, 161–178; b) A. Van Blaaderen, J. Van Geest, A. Vrij, *J. Colloid Interface Sci.* **1992**, *154*, 481–501; c) A. Van Blaaderen, A. Vrij, *J. Colloid Interface Sci.* **1993**, *156*, 1–18.

[9] a) A. Van Blaaderen, A. Vrij, *Langmuir* **1992**, *8*, 2921–2931; b) N. A. M. A. Verhaegh, A. Van Blaaderen, *Langmuir* **1994**, *10*, 1427–1438.

[10] a) S. Santra, J. Xu, K. Wang, W. Tan, *J. Nanosci. Nanotechnol.* **2004**, *4*, 590–599; b) I. Roy, T. Y. Ohulchanskyy, H. E. Pudavar, E. J. Bergey, A. R. Oseroff, J. Morgan, T. J. Dougherty, P. N. Prasad, *J. Am. Chem. Soc.* **2003**, *125*, 7860–7865.

[11] a) C. J. Frederickson, E. J. Kasarskis, D. Ringo, R. E. Frederickson, *J. Neurosci. Methods* **1987**, *90*, 91–103; b) P. D. Zalewski, I. J. Forbes, W. H. Betts, *Biochem. J.* **1993**, *296*, 403–408; c) P. D. Zalewski, I. J. Forbes, R. F. Seamark, R. Borlinghaus, W. H. Betts, S. F. Lincoln, A. D. Wards, *Chem. Biol.* **1994**, *1*, 153–161.

[12] C. J. Fahrni, T. V. O'Halloran, *J. Am. Chem. Soc.* **1999**, *121*, 11448–11458.

[13] M. Montalti, L. Prodi, N. Zaccheroni, A. Zattoni, P. Reschiglian, G. Falini, *Langmuir* **2004**, *20*, 2989–2991.

[14] G. Xue, J. S. Bradshaw, N. K. Dalley, P. B. Savage, R. M. Izatt, L. Prodi, M. Montalti, N. Zaccheroni, *Tetrahedron* **2002**, *58*, 4809–4815.

[15] See for example: a) D. R. Radu, C.-Y. Lai, J. W. Wiench, M. Pruski, V. S.-Y. Lin, *J. Am. Chem. Soc.* **2004**, *126*, 1640–1641; b) D. R. Radu, C.-Y. Lai, K. Jeftinija, E. W. Rowe, S. Jeftinija, V. S.-Y. Lin, *J. Am. Chem. Soc.* **2004**, *126*, 13216–13217.

[16] a) M. Montalti, L. Prodi, N. Zaccheroni, G. Falini, *J. Am. Chem. Soc.* **2002**, *124*, 13540–13546; b) R. Pohl, D. Aldakov, P. Kubát, K. Jursícová, M. Marquez, P. Anzenbacher Jr., *Chem. Commun.* **2004**, 1282–1283; c) M. Arduini, F. Felluga, F. Mancin, P. Rossi, P. Tecilla, U. Tonellato, N. Valentinuzzi, *Chem. Commun.* **2003**, 1606–1607.

[17] W. S. Rasband, ImageJ, U.S. National Institutes of Health, Bethesda, Maryland, USA, http://rsb.info.nih.gov/ij/, **1997–2006**.

[18] G. B. Bachman, G. E. Bennett, R. S. Barker, *J. Org. Chem.* **1950**, *15*, 1278–1284.

[19] *Scientist 2.01*, Micromath Scientific Software, Salt Lake City, **1995**.

Received: May 3, 2006
Revised: July 14, 2006
Published online: December 11, 2006

